NONDESTRUCTIVE EVALUATION OF HARDWOOD LOGS USING AUTOMATED INTERPRETATION OF CT IMAGES

Daniel L. Schmoldt
USDA Forest Service
Brooks Forest Products Center
Virginia Polytechnic Institute and State University
Blacksburg VA 24061-0503

Dongping Zhu
Imatron Industrial Products, Inc.
Foster City CA 94404

Richard W. Conners
Bradley Department of Electrical Engineering
Virginia Polytechnic Institute and State University
Blacksburg VA 24061

INTRODUCTION

Knowledge of internal defects within hardwood logs can be useful even prior to a log's entry into the sawmill. It is in the log yard where the first important decisions are made about processing. First, based upon perceived quality, logs may be sorted as veneer logs or as high-quality sawlogs and sold to domestic veneer mills or for export . Second, roundwood may be bucked into smaller logs to isolate defect areas and to obtain sawlogs with longer sections of clear wood. And third, logs containing metal objects can be identified, thereby preventing headrig saw damage and costly mill down-time.

Inside of the mill, log breakdown can also benefit from internal defect information. Headrig operators require substantial training to become proficient at cutting logs into boards. Experienced saw operators can obtain very good *volume* recovery from many logs by examining external indicators of internal defects and by compensating for external log geometry. As the number of log defects increases, however, it becomes much more difficult to make the best sawing decisions. This is especially true with respect to *value* recovery. Value recovery is much more difficult to accomplish because the quality of final sawn boards must also be considered. By generating 3-dimensional transparent images of logs, we can give the saw operator valuable information that can greatly improve the total value of boards cut from logs. We are engaged in other research that aims to make actual sawing decisions based on log defect information. In this case, rather than just display an internal picture of a log to the saw operator, we can tell the operator exactly how to cut the log, or even control the positioning and sawing of the log automatically.

Nondestructive evaluation techniques attempt to examine some object of interest by scanning in a manner that does not disrupt the physical or structural integrity of the material.

Review of Progress in Quantitative Nondestructive Evaluation, Vol. 12
Edited by D.O. Thompson and D.E. Chimenti, Plenum Press, New York, 1993

Most scanning methods bombard a specimen with energy, either in the form of sound waves or electromagnetic waves. Detectors measure the energy emitted by the specimen, and from this information various characteristic of the object material can be inferred. Computerized tomography (CT) measures the attenuation of x-ray energy as it passes through a plane of the object specimen. By taking successive 2-d images, or tomographs, it is possible to determine the internal appearance of the object. This technique was first applied in medical applications [1].

Chemical similarities between human specimens and wood led researchers to consider CT scanning of wood objects. A number of investigations have examined the quality of CT images and their use for wood density and moisture content estimates and for the identification of internal structures [2, 3, 4, 6, 7, 11, 13, 15, 18]. These investigators have found that CT images provide a large amount of information about the internal characteristics of wood. Even for large objects, such as logs, internal structures are readily visible to someone examining a tomograph.

It is unrealistic, however, to expect anyone to gain much insight into the 3-d appearance of an entire log interior by viewing a sequence of 2-d CT images. Rather, these cross-sectional images must be combined to form a solid geometry view of the log and its internal features. Consequently, researchers have begun to develop automated methods for interpreting CT images of logs [8, 10, 12, 23, 24]. Once different internal log features can be automatically detected then it becomes a relatively straightforward task to integrate those views into a 3-d rendering of the log.

Because we are continuing to develop the machine vision software to automatically interpret CT images, a large and comprehensive data base of CT images is critical. These data collection procedures are outlined in the next section. Following this, a brief description of our machine vision system is presented. Some preliminary defect recognition results indicate the feasibility of this approach and suggest possible modifications to our present methods.

CT IMAGE DATA BASE

Theoretically, x-ray attenuation is affected by the density of the material through which the rays pass. Empirical evidence demonstrates that this relationship is very linear in woody materials [7, 18]. Each pixel (a small area in the CT image that actually represents a small volume, or voxel) of a CT image has an associated CT number which describes that volume's attenuation of transmitted x-rays, relative to the attenuation of a similar volume of water. Because knots, bark, rot, sapwood, heartwood, voids, etc. have different densities or density patterns, CT numbers can be used to distinguish these log defects.

Data Collection

At the beginning of our research on automated interpretation of CT images there was only one database of CT images of hardwood logs available. The database was the one created to perform the research reported in [21]. While this database contains a large number of CT slices, those slices only represent a few defects examples. To address this paucity of data, a new CT image database was created for use in our image interpretation research.

First, collecting CT imagery of logs, or for that matter anything else, is very expensive. Hence, it is very important that each slice provide as much useful information as possible. For the purposes of developing a computer vision system the "important" information contained in each slice of CT imagery is the way different defects manifest themselves in relation to one another and to clear wood. Hence, low grade logs were individually selected for use in creating the database and only defected sections of these logs were used to create our data base.

To provide some information about the variations caused by interspecific differences in hardwoods, two species were selected for consideration, red oak, a high value ring-porous

species, and yellow poplar, a low value diffuse-porous species. The CT scanner used was a Siemens Somaton DR2 system present at a local hospital. Slice spatial resolution was 2.5 X 2.5 millimeters within a slice plane and 8 millimeters in thickness. Each slice represented a 256X256 image with 12 bits of CT number information.

After the sections were scanned they were returned to cold storage. Within a very few days each section was removed from cold storage and was cutup into very thin slices using a Woodmizer saw. Each of these wood slices corresponded as closely as was possible to the CT image slices taken by the Siemens scanner. Each thin slice was labeled, cleaned, bagged with the other thin slices cut from the same section, and returned to cold storage. The goal was to perform all this additional processing without drying out the thin wood slices.

The last step involved in creating the CT image database was to take a color photograph of each thin wood slice. Appearing in each photograph is information that allows one to determine the CT slice number for which this thin wood slice corresponds, the log section from which the thin slice was cut, the log from which this log section was cut, and the species of this log. The film negative and a 5 X 7 color print of each thin wood slice have all been saved for archival purposes. A total of 490 CT image slices, color photographs, and film negatives comprise this image database.

AUTOMATED INTERPRETATION

To provide defect information based on CT images, however, requires that we have vision software to interpret those individual images. A machine vision system must distinguish defects from clear wood, must label the different defect areas, and must integrate 2-d CT slices to create 3-d defect objects. Typical mill operations also require that such a vision system deal with a variety of species and with logs of varying condition. To accommodate these requirements, the defect recognition system must incorporate robust methods that have been developed using extensive data sets of different hardwood species and log conditions.

Image Analysis

The original 12-bit CT images of hardwood logs contain several types of pixels, such as air (background), clear wood, knots, splits, bark, and so on. In addition, there is a textural structure on each of the CT images that represents the annual ring structure of tree growth. These fine rings are visible both in the sapwood and heartwood, and they tend to grow in the same textural pattern or directionality. To effectively distinguish defects from clear wood and air, we found it necessary to eliminate these annual rings before segmenting an image into a number of uniform regions.

A modification of Unser's 2-d adaptive filter [27], called 3-d adaptive filtering [25], was applied to each of the tomographs to eliminate annual ring structures. This filter locally optimizes a least squares error criterion and provides estimates of the coefficients $a_{i,j,k}$ and $b_{i,j,k}$ in the following expression:

$$z_{i,j,k} = a_{i,j,k}x_{i,j,k} + b_{i,j,k}y_{i,j,k} \quad (1)$$

where $z_{i,j,k}$ is the true image signal at point (i, j, k), $x_{i,j,k}$ is the original noisy signal, and $y_{i,j,k}$ is a filtered version of the noisy signal. Filtering is performed using a small volume around each pixel that includes neighboring pixels on adjacent CT images. The least squares procedure adjusts the weights $a_{i,j,k}$ and $b_{i,j,k}$ according to the amount of image degradation filtering produces. As filtering increases the regression error beyond the background error, the weight $a_{i,j,k}$ increases and $b_{i,j,k}$ decreases in order to retain the original signal and to down weight the filtered one.

Images that have been filtered using the 3-d adaptive filter are thresholded on an image-by-image basis using a multiple threshold scheme [23]. First, a histogram is computed from the filtered image and smoothed using a Gaussian function. Because bark and knots have

similar CT values, they are temporarily treated like a single type of defect. Accordingly, three thresholds $\{T_1, T_2, T_3\}$ are determined from the smoothed histogram. These thresholds segment each CT image into a number of uniform regions. Thresholds are determined as follows:

T_1: the location of the first zero crossing of the histogram's slope after T_0,

T_2: the location of the maximum change in the slope of the histogram,

T_3: the location of the penultimate zero crossing of the histogram's slope.

The specification of T_0 truncates the histogram by removing background (air) pixels. A typical histogram with threshold points appears in Figure 1.

Image gray-level thresholds produce a number of regions that represent potential defects. It also creates, however, a small number of spurious defect regions. To make subsequent defect recognition methods more effective, spurious regions need to be removed. Consequently, morphological operations, such as erosion and dilation, are applied to the segmented image. In our vision system, an image erosion operation is first performed on the segmented image to remove the small spurious areas. Then image dilation is performed to restore those pixels of the real defect regions that have been eliminated by the erosion operation. These operations eliminate spurious regions and smooth defects.

The processes of filtering, segmentation, and smoothing produce a number of uniform regions on each image which, when grouped together in 3-d, represent different internal log structures. In 3-d, a knot would appear like a paraboloid, bark like a generalized cylinder, a hole like a cylinder, and a split like a ribbon, etc. To identify the proper 3-d volumes of potential defects, pixels with similar CT attributes on a number of segmented images are grouped into connected volumes, according to 6-or 18-neighborhood connectiveness in 3-d [24].

Scene Analysis

The purpose of the scene analysis module is to extract distinguishing features from processed CT tomographs and use them to categorize various defects. Given the characteristics of wood defects, statistical or analytical classification procedures alone are difficult to implement successfully. Less exacting methods seem better suited to this type of problem. A heuristic, rule-based recognition system was used by [26] to identify defects in sawn lumber. A similar method has been applied in this study.

For each of the 3-d volumes detected by the above volume growing process, statistical, geometric, and topological features are readily computed from the 3-d image data. Currently, 5 basic descriptors have been derived to enhance the separability of internal log features. Additional descriptors can be added to the system as additional defects need to be recognized or as current defects need to be distinguished more accurately. The following are brief explanations of the descriptors that may be computed from a sequence of images:

(1) The mean value (MEAN) - This feature is obtained by finding the mean CT values for all pixels contained in a volume. Because knots are denser than clear wood, knots attenuate x-rays more and therefore have a higher CT value. This is an important feature to identify dense defects.

(2) The variance value (VAR) - Sample variance of a volume is calculated from all pixel values in the volume. This is a useful feature to distinguish bark from knots because they have different variance values.

(3) The minimum distance (DIST) - This is taken as the distance from the centroid of a volume to the Z-axis. Bark (except for included bark pockets) is a great distance from the center of the log, therefore, it has a large DIST value.

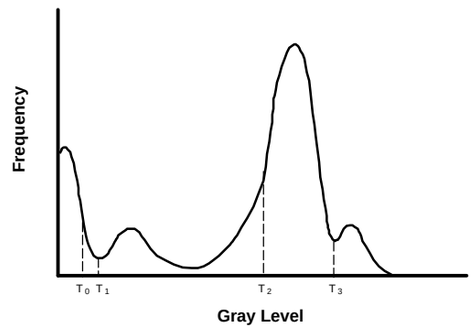

Figure 1. A typical gray-level histogram of a CT image contains several landmark features $\{T_1, T_2, T_3\}$that can be used to separate pixels into likely defect (knots, bark, voids) and non defect (clear wood) categories.

(4) The predicate (TOUCH) - This is a binary predicate with value 1 or 0. A value of 1(O) indicates a volume touching (not touching) the background (air). Since knots usually do not touch air, this is a good feature to differentiate knots from other objects.

(5) The Volume (VOLM) - This is the 3-d volume occupied by an object. Clear wood has a much larger volume than any other object in a log, while splits and holes have a much smaller volume than other defects.

From the population distribution of a given feature, we can derive threshold values that separate the population of values into discrete classes. Threshold values are determined visually from the peaks and valleys of the histogram that is derived from a training set of CT images. Linguistic qualifiers, such as "high" and "low", label these feature value classes. An *evidence function*, expressed as a discrete or continuous step function, is used to relate linguistic qualifiers and levels of evidence for various defects. Figure 2 illustrates three examples of such evidence functions *f(v)* for feature *v = VAR* applied to defects bark, knots, and clear wood.

These evidence functions are implemented as a set of rules (or critic) for each feature. Each critic votes for the classification of each internal log structure. A production system was built to consider each feature-linguistic qualifier pair separately. The action of a rule is to contribute positive evidence (1.0) to classes in which the feature is usually present, negative evidence (-1.0) to those in which it is usually absent, and no evidence (0.0) to the rest. To accommodate situations where a feature is present occasionally and absent at other times, partial evidence (0.5, -0.5) assignment is permitted. The defect class that receives the highest total vote over all critics becomes the classification for that log structure. The functions in Figure 2 could be represented by the following three rules:

```
if VAR = L then  conf(bark, -1.0)
                 conf(knot, 0.5)
                 conf(wood, 1.0).
if VAR = M then conf(bark, 0.5)
                 conf(knot, 1.0)
                 conf(wood, 0.5).
if VAR = H then conf(bark, 1.0)
                 conf(knot, 0.5)
                 conf(wood, -1.0).
```

This is in fact a voting process where a more influential vote is given to strong evidence and less influence to weak evidence. Some image interpretation results based on these image and scene analysis methods are presented in the next section.

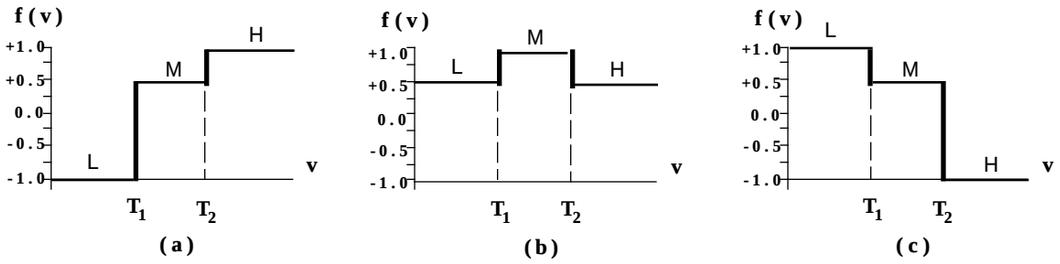

Figure 2. An evidence function *f(v)* relates discrete values (L, M, H) for feature *v = VAR* with evidence values for the defect bark (a). Knots (b) and clear wood (c) have different evidence functions. The threshold values, T_1 and T_2, are unrelated to the multiple threshold values used in segmentation and were established from the distribution of *VAR* values in a training set.

RESULTS

Experiments were conducted using the above described approaches to process CT images and to recognize wood defects from several red oak and yellow poplar logs. A small set of CT slices were selected from a sequence of the log images as the training data. Feature distributions computed from this training set defined a set of threshold values that were used to determine linguistic qualifiers for each feature. Rules were then applied to individual object volumes to assign confidence values to different defect class hypotheses. Adding up the confidence values contributed to a volume by all rules, the object was assigned the class that had the highest total confidence value. Figure 3 illustrates some results on four consecutive slices of a yellow poplar log.

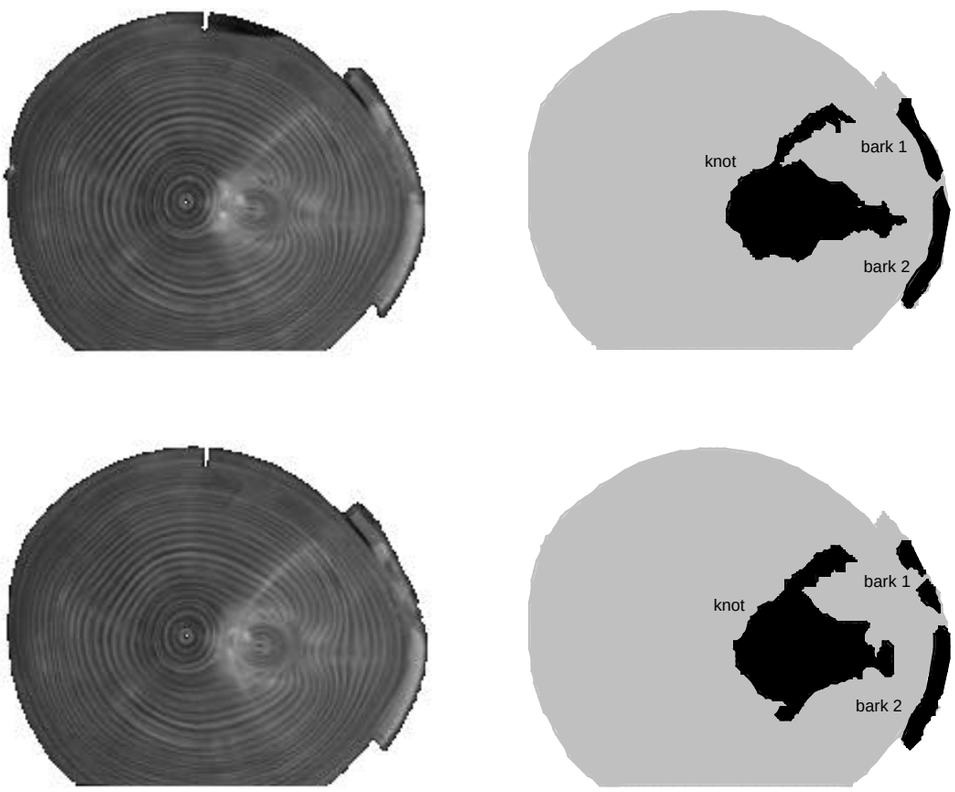

Figure 3. Original CT images and defect recognition results are depicted using four consecutive slices from a yellow poplar log.

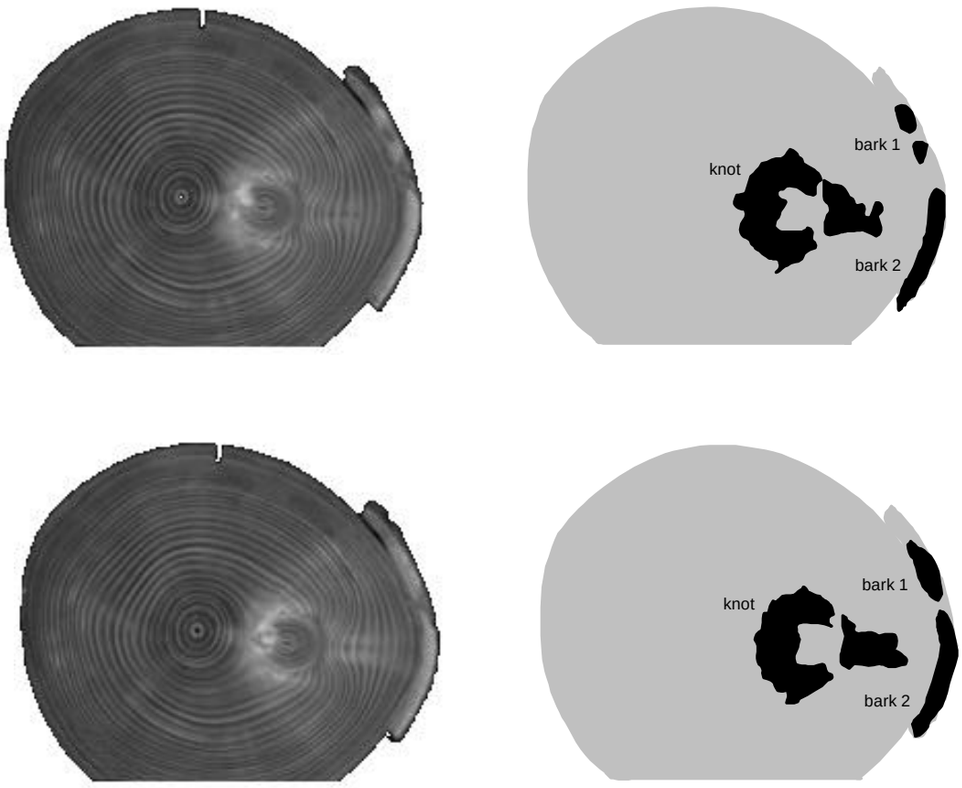

Figure 3. Original CT images and defect recognition results are depicted using four consecutive slices from a yellow poplar log.

CONCLUSIONS AND DISCUSSION

Several questions need to be resolved before we can claim that this image interpretation software operates successfully. First, the system must perform better on the slices of red oak and yellow poplar that we currently have in our database. We suspect that some of these problems are related to varying moisture content. Second, our software must be tested and validated on other species and on logs of differing condition. Third, we have not yet performed any tests of software speed. Initial image processing steps are computationally intensive while the later recognition steps are relatively simple and fast. Fourth, to apply this internal defect information to subsequent log processing decisions we must be able to accurately circumscribe defects. Under- or over-estimating defect size will drastically reduce the efficacy of subsequent processing decisions. Fifth, alternative image and scene analysis methods that utilize texture information may be required for more accurate defect labeling and sizing. The ability to answer each of these questions can benefit from an expanded database of CT images and their ground truth records.

Log moisture content complicates the image processing stage because it confounds density measures [3, 8]. For example, low-density areas such as rot or bark may, when they are wet, attenuate x-rays similarly to dry heartwood. Information about an internal region's shape, orientation, texture, and size must also be considered to correctly identify a particular region as defect or clear wood [8, 23]. It is not currently known, however, in what way the masking effect of moisture content varies across species and defect types and how automated interpretation methods can best deal with this image noise.

CT scanners are limited in speed by each of their two operations, x-ray scanning and image reconstruction. Recent developments, however, have reduced the fastest scan time so that up to 34 images per second can be captured using an ultra-fast medical scanner [17, 21]. A mobile, industrial scanner is currently available that can perform both scanning and

reconstruction in an average time of 1 image per second (Scot Land, personal communication). While this rate still does not permit intensive scanning of all logs at a mill, if used wisely (e.g., on high-value logs and only on defect areas of logs), the current generation of CT scanners can increase sawmill profitability.

REFERENCES

1. P. E. New, W. R. Scott, J. A. Schnur, K. R. Davis, and J. M. Taveral, Radiology 110, 109 (1974).
2. D. M. Benson-Cooper, R. L. Knowles, F. J. Thompson, and D. J. Cown, New Zealand Service, Bull. No. 8 (Forest Research Institute, 1982).
3. R. Birkeland, and S. Halogen, in *Proceedings of the 2nd International Conference on Scanning Technology in Sawmilling* (Forest Industries/Wood World, San Francisco, 1987).
4. A. E. Burgess, in *Proceedings of the 1st International Conference on Scanning Technology in Sawmilling* (Forest Industries/Wood World, San Francisco, 1985).
5. S. J. Chang, in *Proceedings of the 3rd International Conference on Scanning Technology in Sawmilling* (Forest Industries/Wood World, San Francisco, 1989).
6. D. J. Cown, and B. C. Clement, Wood Science Technol. 17, 91 (1983).
7. J. R. Davis, and P. Wells, Industrial Metrology 2, 195 (1992).
8. B. V. Funt, and E. C. Bryant, Forest Prod. J. 37, 56 (1987).
9. D. G. Hodges, W. C. Anderson, and C. W. McMillin, Forest Prod. J. 40(3), 65 (1990).
10. F. Hopkins, I. L. Morgan, H. Ellinger, and R. Klinksiek, Materials Evaluation 40, 1226 (1982).
11. T. L. Laufenberg, Forest Prod. J. 36(2), 59 (1986).
12. C. W. McMillin, Wood Science 14(3), 97 (1982).
13. W. H. Miller, Nucl. Instrum. Meth. in Physics Res. 270, 590 (1988).
14. P. E. New, W. R. Scott, J. A. Schnur, K. R. Davis, and J. M. Taveral, Radiology 110, 109 (1974).
15. M. Onoe, J. W. Tsao, H. Yamada, H. Nakamura, J. Kogura, H. Kawamura, and M. Yoshimatsu, Nucl. Instum. Meth. in Physics Res. 221, 213 (1984).
16, D. B. Richards, W. K. Adkins, H. Hallock, and E. H. Bulgrin, USDA Forest Service Research Paper FPL-356 (1980).
17. F. L. Roder, E. Scheinman, and P. Magnuson, in *Proceedings of the 3rd International Conference on Scanning Technology in Sawmilling* (Forest Industries/Wood World, San Francisco, 1989).
18. P. A. Shadbolt, M.S. Thesis, Chisholm Institute of Technology, 1988 (unpublished).
19. J. A.Tsolakides, Forest Prod. J. 19(7), 21 (1969).
20. F. G. Wagner, T. E. G. Harless, P. H. Steele, F. W. Taylor, V. Yadama, and C. W. McMillin, in *Proceedings of Process Control/Production Management of Wood Products: Technology for the 90's* (The University of Georgia, Athens GA, 1990), p. 77.
21. F. G. Wagner, F. W. Taylor, D. S. Ladd, C. W. McMillin, and F. L. Roder, Forest Prod. J. 39(11/12), 62 (1989).
22. F. G. Wagner, F. W. Taylor, P. Steele, T. E. G. Harless, in *Proceedings of the 3rd International Conference on Scanning Technology in Sawmilling* (Forest Industries/Wood World, San Francisco, 1989).
23. D. Zhu, R. W. Conners, F. Lamb, D. L. Schmoldt, and P. A. Araman, in *Proceedings of the 4th International Conference on Scanning Technology in Sawmilling* (Forest Industries/Wood World, San Francisco, 1991).
24. D. Zhu, R. W. Conners, D. L. Schmoldt, and P. A. Araman, in *Proceedings of the 1991 IEEE International Conference on Systems, Man, and Cybernetics*, p. 173.
25. D. Zhu, R. W. Conners, and P. A. Araman, in *Proceedings of the 1991 IEEE International Conference on Systems Engineering*, p. 457.
26. T. H. Cho, R. W. Conners, and P. A. Araman, in *Proceedings of the 1990 IEEE International Conference on Systems, Man, and Cybernetics*, p. 345.
27. M. Unser, Signal Processing 20, 3 (1990).